

Stripe segregation and magnetic coupling in the nickelate $\text{La}_{5/3}\text{Sr}_{1/3}\text{NiO}_4$

Udo Schwingenschlög^{1,2,*}, Cosima Schuster¹, and Raymond Frésard³

¹Institut für Physik, Universität Augsburg, 86135 Augsburg, Germany

²KAUST, PCSE Division, P.O. Box 55455, Jeddah 21534, Saudi Arabia

³Laboratoire CRISMAT, UMR CNRS-ENSICAEN(ISMRA) 6508, and IRMA, FR3095 Caen, France

Received 23 January 2009, accepted 14 February 2009 by U. Eckern

Key words Diagonal filled stripes, structure relaxation, electronic structure.

PACS 71.20.-b, 71.45.Lr, 75.25.+z

We investigate the consequences of the stripe formation in the nickelate $\text{La}_{5/3}\text{Sr}_{1/3}\text{NiO}_4$ for the details of its crystal structure and electronic states. Our data are based on numerical simulations within density functional theory (DFT) and the generalized gradient approximation (GGA). The on-site Coulomb interaction is included in terms of the LDA+U scheme. Structure optimization of preliminary experimental data indicates a strong interaction between the structural and electronic degrees of freedom. In particular, we find a segregation of the diagonal filled stripes induced by a delicate interplay with the magnetic coupling. Beyond the cooperative effect of stripe segregation and spin order, distinct octahedral distortions are essential for the formation of an insulating state.

1 Introduction

Doped Mott insulators present a wealth of intriguing properties with a great potential for technological applications. They are either based on metallicity, like high- T_c superconductivity and thermoelectricity, or trace back to an insulating behavior, like colossal magneto-resistance and multiferroics. Therefore, understanding the origin of the insulating state of these doped Mott insulators has clear implications, be it caused by a lack of coherence [1] or by a formation of an inhomogeneous state, as a stripe phase, for instance [2–8]. Though intensely debated, see Ref. [9] for a review, there is growing consensus that electronic models can account for the poorly metallic character of the diagonal filled stripes observed in cuprates, almost irrespective of their microscopic structure. For instance, magnetic diagonal filled stripe phases of the Hubbard model are insulating [10], while a poorly metallic phase with nodal quasiparticles characterizes flux diagonal filled stripe phases of the $t - J$ model [11]. In contrast, similar model calculations devoted to isostructural nickelates fail to reproduce an insulating groundstate [12].

Experimentally, the stripe order in $\text{La}_{2-x}\text{Sr}_x\text{NiO}_4$ and $\text{Nd}_{2-x}\text{Sr}_x\text{NiO}_4$ has been evidenced by spin-polarized as well as unpolarized neutron scattering. With decreasing temperature, the appearance of peaks at the wave vectors $\mathbf{Q}_c = 2\pi(\epsilon, \epsilon)$ and $\mathbf{Q}_s = \pi(1 \pm \epsilon, 1 \pm \epsilon)$, respectively, with $\epsilon \simeq x$, is interpreted as onset of a diagonal filled stripe. The onset temperature is sensitive to the doping, turning out to have a maximum at $x = 1/3$, i.e. when the charge wave vector matches right the spin wave vector. In this case, specific heat [13], transport [14], and optical conductivity [15] data point to an ordering temperature of $T \sim 240$ K. Recently, the stability of the stripe phase has been further probed via non-linear transport experiments for

* Corresponding author E-mail: udo.schwingenschloegl@physik.uni-augsburg.de

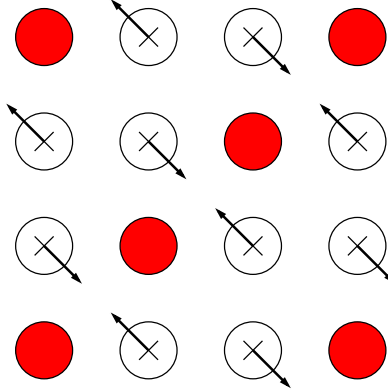


Fig. 1 Schematic representation of the NiO_2 -layer in $\text{La}_{5/3}\text{Sr}_{1/3}\text{NiO}_4$ highlighting the diagonal Ni stripes. O atoms are not shown for clarity. Arrows indicate the principal structural distortion consistent with AF spin order.

the system $\text{Nd}_{1.67}\text{Sr}_{0.33}\text{NiO}_4$ [16]. No depinning of the stripes has been observed: instead, the non-linear transport is attributed to resistive heating, thereby pointing towards a rather robust insulating state.

On the theoretical side, quite some efforts have been made to properly describe these materials, especially by the investigation of realistic models. While an extensive study of a two-band Hubbard model for the e_g electrons correctly predicts diagonal filled stripes to be lowest in energy within this class of states, the groundstate is still metallic [12]. Adding electron-lattice coupling promotes the insulating groundstate, but the available results are limited to the $x = 1/2$ case and to particular lattice distortions [17]. Band structure calculations also have been performed [18, 19]. However, because they make use of an explicit lattice structure as input, which so far could not be determined experimentally for the title compound, the validity of the calculations could be limited. Indeed, as argued in [17], a strong spin-charge-lattice coupling is to be anticipated in layered nickelates. Using a two-band Hubbard model, Hotta and Dagotto [20] have demonstrated the interplay of Coulombic and phononic interactions and its relevance for the stripe formation.

Another appealing scenario of spin-lattice interaction is sketched in Fig. 1, where we show the Ni atoms for a NiO_2 -layer. Atoms along the stripes and in the magnetic domains are represented by full and open circles, respectively. A Ferromagnetic (F) as well as an antiferromagnetic (AF) order between the spins on the stripe and the domain sites is compatible with the experimental modulation vector $\mathbf{Q}_s = \pi(2/3, 2/3)$. For the AF alignment, the structural distortion shown in Fig. 1 enhances the superexchange over the stripes significantly, while it reduces the frustrated superexchange within the magnetic domains only moderately. The configuration thus is expected to be subject to an instability against a modulation of the Ni–Ni bond length perpendicular to the stripe direction. In contrast, the F alignment in this respect is consistent with an equal spacing of the Ni atoms, because a modulation of the bond lengths tends to reduce the kinetic energy. The competition between the two states makes it highly desirable to understand in detail the shape of the lattice deformations encountered in the system, and their consequences for the electronic structure.

2 Technical details

To that aim we have performed band structure calculations for the $x = 1/3$ compound $\text{La}_{5/3}\text{Sr}_{1/3}\text{NiO}_4$. Our following considerations first focus on the lattice deformations tracing back to the stripe formation, where the parent body-centered tetragonal K_2NiF_4 structure with space group $I4/mmm$ will act as a reference frame [21]. Lattice deformations have not been reported in the literature so far, because the

abbreviation	intraplane spin alignment	interplane spin alignment
ADFAS	F	AF
CDFAS	AF	F
GDFAS	AF	AF

Table 1 Definitions of the A-, C-, and G-type D(iagonal) F(illed) A(ntiferromagnetic) S(tripe) spin configurations.

experimental refinement of the crystal structure has concentrated on the lattice parameters. In fact, refinement of the atomic positions is difficult without a proper structure model, which, finally, is provided by our structure optimization data. As second step, we analyze the electronic properties of the system for different spin configurations, which allows us to determine the magnetic groundstate of various diagonal filled antiferromagnetic stripes. The spin configurations under investigation are defined in table 1. In addition, the CDFAS and GDFAS patterns are illustrated in Fig. 2.

In our electronic structure calculations we use density functional theory (DFT) as implemented in the Wien2k code [22]. The latter is appropriate for the present investigation, because it allows us to perform a full structure optimization for a complex material with large unit cell [23] and to account for the electronic correlations present in the system, by the LDA+U (local density approximation plus on-site Coulomb interaction) method [24]. For the structure optimizations the generalized gradient approximation (GGA) [25] and for the LDA+U calculations the self-interaction correction (SIC) [26, 27] is used.

The tetragonal $\text{La}_{2-x}\text{Sr}_x\text{NiO}_4$ unit cell resulting from the parent $I4/mmm$ lattice contains two formula units. It is very convenient to describe the atomic arrangement in terms of parallel layers of NiO_6 -octahedra, separated by the La/Sr atoms. To be specific, we have NiO_2 -layers parallel to the ab -plane of the tetragonal unit cell, consisting of a square planar lattice of Ni atoms, and O atoms located midway between them. Due to the stripe charge order, we have two crystallographically inequivalent NiO_2 -layers comprising the metal sites Ni1/Ni3 and Ni2/Ni4, respectively. For further details on the crystal structure, the supercell setup, as well as other technical aspects, we refer the reader to Ref. [19]. We use the setup described therein as the starting point of our present study. However, our new calculations thoroughly take into account the structure relaxation induced by the stripe charge order. To this end, we optimize the atomic positions individually for all spin patterns under consideration.

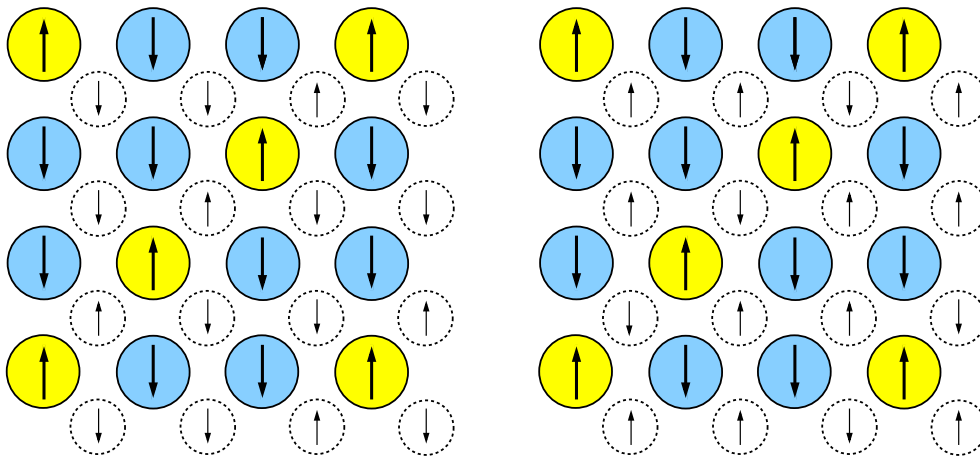


Fig. 2 Magnetic structure of the Ni atoms in the NiO_2 -layers of $\text{La}_{5/3}\text{Sr}_{1/3}\text{NiO}_4$ for the CDFAS (left hand side) and GDFAS (right hand side) spin configurations. Full yellow (blue) circles denote the Ni1 (Ni3) atoms, whereas dashed circles refer to the second NiO_2 -layer, containing the Ni2 (Ni4) atoms, see the text.

3 Results and discussion

Turning to the data obtained from our structure optimizations, we first mention that the NiO_6 -octahedra of $\text{La}_{5/3}\text{Sr}_{1/3}\text{NiO}_4$ are elongated and tilted with respect to the c -axis of the tetragonal unit cell [28, 29]. While structure distortions, in general, are tiny for the ADFAS pattern, we observe a sizeable response of the NiO_6 -octahedra to the charge order for both the CDFAS and GDFAS pattern, i.e. for AF intraplane magnetic coupling. The fact that the latter distortions are closely related to each other supports our initial speculations about a strong spin-lattice interaction. We summarize the observed apical and equatorial Ni–O bond lengths in the four inequivalent NiO_6 -octahedra in Table 2, revealing significant deviations from the ideal values of 2.21 Å and 1.92 Å, respectively. The distortion associated with these values is illustrated in Fig. 3 for the Ni2/Ni4-plane, where the shifts off the symmetric positions have been magnified by a factor of 4. The pattern is similar for the Ni1/Ni3-plane, which is obtained by shifting the Ni2/Ni4-plane by the vector $(a/2, 0, c/2)$. While for stripe ordered $\text{La}_{1.875}\text{Ba}_{0.125}\text{CuO}_4$ [30], for example, a modulation of the La ions is reported, such displacements are negligible in our case for both the La and Sr sites.

Whereas a strong relaxation of the structure has to be expected for a NiO_6 -octahedron, we additionally observe a characteristic relaxation pattern for the Ni sublattice, see the schematic illustration in Fig. 1. With respect to the (highlighted) diagonal stripes, neighboring Ni atoms are subject to displacements towards

atom	apical Ni–O bond length (Å)	equatorial Ni–O bond length (Å)
Ni1	2.17 (2×)	1.94 (4×)
Ni2	2.23 (2×)	1.94 (4×)
Ni3	2.20 (2×)	1.89 (2×) and 1.92 (2×)
Ni4	2.24 (2×)	1.88 (2×) and 1.94 (2×)

Table 2 Bond lengths in the NiO_6 -octahedra obtained for AF intraplane magnetic coupling (CDFAS/GDFAS).

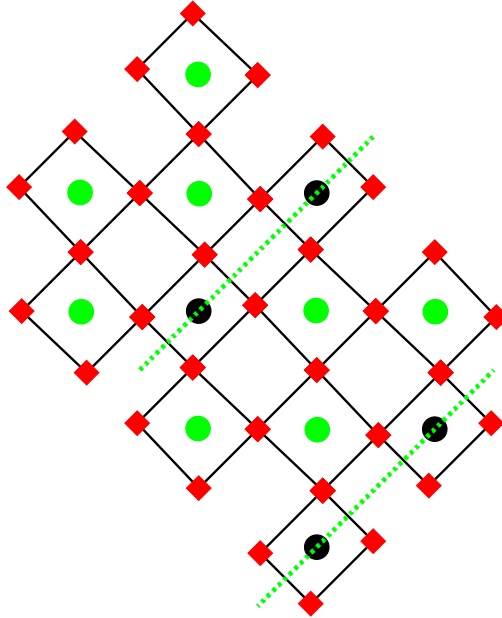


Fig. 3 Optimized crystal structure of a NiO_2 -layer in $\text{La}_{5/3}\text{Sr}_{1/3}\text{NiO}_4$. The Ni2 (Ni4) and O sites are represented by black (green) circles and diamonds, respectively, and stripes by dotted lines.

atom moving	towards	displacement (\AA)		
		ADFAS	CDFAS	GDFAS
Ni3	Ni1 chain	0.0002	0.0065	0.0016
Ni4	Ni2 chain	0.0032	0.0114	0.0300

Table 3 Atomic displacements as obtained from the structure optimizations for the different spin patterns. The values refer to the relative shift of a Ni3/Ni4 site towards the chain formed by the Ni1/Ni2 sites within a NiO₂-layer.

them. To be specific, all shifts are oriented perpendicular to the stripe direction and parallel to the basal plane of the tetragonal unit cell, thus parallel to the NiO₂-layers. Their absolute values are summarized in Table 3. The distortion pattern of the Ni sublattice is well described in terms of a segregation of neighboring stripes. By this mechanism, the magnetic intraplane interaction is enhanced within the magnetic domains. After all, this is advantageous for the AF configuration only, since the F configuration is predominantly promoted by local processes. Furthermore, our line of reasoning is fully consistent with the fact that F intraplane coupling does not result in a significant structure relaxation.

Concerning the electronic states, structural relaxation has serious effects. In contrast to experimental findings, previous calculations for the non-optimized geometry resulted in metallic solutions with broad conduction bands [19]. This behavior appeared to be characteristic for all spin configurations involving parallel spins along the stripes, particularly for our ADFAS, CDFAS, and GDFAS patterns. An insulating band gap is observed only for spin configurations involving antiparallel spins along the stripes [18]. While the density of states (DOS) for the ADFAS phase is subject to only small changes, the structure optimizations for the CDFAS/GDFAS phase yield substantial alterations. The associated spin-polarized partial Ni 3d DOS, split up into contributions from the four inequivalent Ni atoms, is depicted in Fig. 4. These results are based on the LDA+U scheme, with local interactions on all Ni sites. For the on-site Coulomb interaction we set $U = 8$ eV and for the Hund's rule coupling $J_H = 0.8$ eV [31, 32].

Fig. 4 seems to indicate the formation of an insulating band gap, as the consequence of a separation of valence bands just above the Fermi energy. Closer inspection of the band structure, however, shows that this splitting is incomplete, which could be attributed to the fact that the on-site interaction has not been taken into account in the structure optimizations, for technical reasons. Nevertheless, it is clear that the

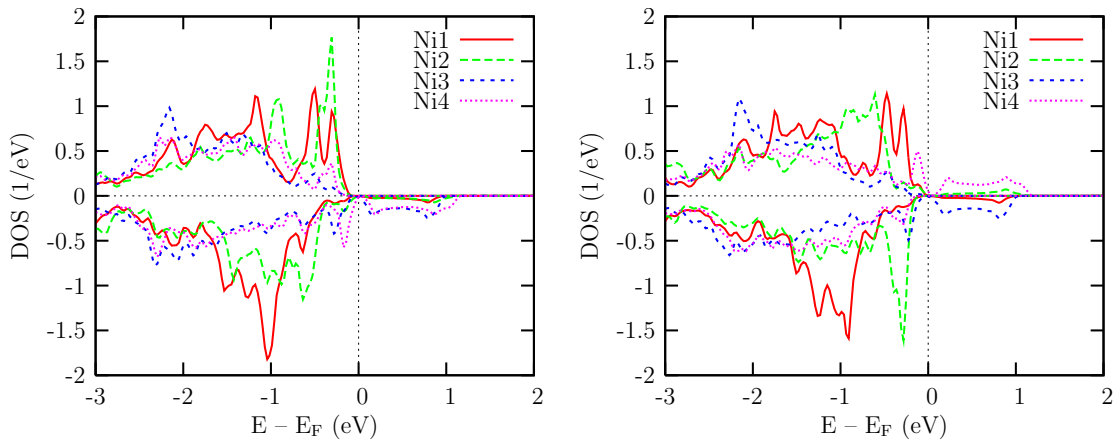


Fig. 4 Partial spin majority and minority Ni 3d DOS (per atom) for the four inequivalent Ni sites in the CDFAS (left hand side) and GDFAS (right hand side) spin patterns of La_{5/3}Sr_{1/3}NiO₄.

U (eV)	J_H (eV)	total energy gain (mRyd)		
		ADFAS	CDFAS	GDFAS
0	0	8.7	19.5	17.3
8	0.8	163	156	157

Table 4 Total energy gain per Ni atom resulting from the spin-polarization and the simultaneous structural distortion. Values are compared for GGA and LDA+U calculations, and for the ADFAS, CDFAS, and GDFAS spin patterns.

formation of an insulating state is intimately connected to the relaxation of the O octahedra and the stripe segregation.

For the optimized crystal structures, we now compare the spin patterns under consideration from the energetic point of view. The energy gain (with respect to the paramagnetic energy calculated for the non-optimized $\text{La}_{5/3}\text{Sr}_{1/3}\text{NiO}_4$ structure) of the magnetic solutions is summarized in Table 4. In addition to the solutions displayed in Fig. 4, it seems to be possible to obtain metallic solutions with similar energies. However, they are more indicative of a poor convergence than a physically relevant result. All magnetic phases are lower in energy than the paramagnetic phase, already for $U = 0$. In this case, the largest total energy gain amounts to 19.5 mRyd per Ni atom for the CDFAS phase. However, on inclusion of the on-site Coulomb interaction the energy order is inverted, which contradicts the experimental situation. The ADFAS pattern now is favored by 6 mRyd per Ni atom, while the CDFAS and GDFAS configurations are almost degenerate. Since the energy differences of the various phases are rather small, this fact again is explained by the interplay between the magnetic ordering and details of the crystal structure. Probably, a structure optimization within the LDA+U scheme is required to restore the original energy order.

4 Conclusions

In conclusion, we have presented DFT calculations for the nickelate $\text{La}_{5/3}\text{Sr}_{1/3}\text{NiO}_4$. Optimization of the crystal structure results in two characteristic types of lattice distortions: (1) Distinct deformations of the NiO_6 octahedra pave the way for the opening of an insulating gap, which, so far, could not be reproduced assuming parallel spins along the stripes. (2) The strong spin-lattice interaction induces a segregation of neighboring diagonal filled stripes, as the deformation cooperates with the AF interaction perpendicular to the stripes. This new mechanism of stripe segregation is expected to be relevant for a large class of striped materials with related crystal structures. Moreover, neither the distortions of the O nor of the Ni sublattice further reduce the symmetry initially imposed by the charge pattern. Stripe ordered $\text{La}_{5/3}\text{Sr}_{1/3}\text{NiO}_4$ thus maintains a $Cmmm$ lattice symmetry, which to verify is an important task for future experiments. Besides, there is a clear need for structure optimization on the LDA+U level, to enable a more reliable discussion of the stability of the various phases. Work along these lines is in progress.

Acknowledgements We acknowledge fruitful discussions with T. Kopp, M. Raczkowski, and Y. Sidis. Financial support was provided by the Deutsche Forschungsgemeinschaft (SFB 484) and the Bayerisch-Französische Hochschulzentrum.

References

- [1] B. Kyung, S.S. Kancharla, D. Sénéchal, A.-M. S. Tremblay, M. Civelli, G. Kotliar, Phys. Rev. B **73**, 165114 (2006).
- [2] V. Sachan, D.J. Buttrey, J.M. Tranquada, J.E. Lorenzo, and G. Shirane, Phys. Rev. B **51**, 12742 (1995).
- [3] J.M. Tranquada, D.J. Buttrey, and V. Sachan, Phys. Rev. B **54**, 12318 (1996).
- [4] S.-H. Lee and S.-W. Cheong, Phys. Rev. Lett. **79**, 2514 (1997).
- [5] H. Yoshizawa, T. Kakeshita, R. Kajimoto, T. Tanabe, T. Katsufuji, and Y. Tokura, Phys. Rev. B **61**, R854 (2000).

- [6] S.-H. Lee, J.M. Tranquada, K. Yamada, D.J. Buttrey, Q. Li, and S.-W. Cheong, Phys. Rev. Lett. **88**, 126401 (2002).
- [7] P.G. Freeman, A.T. Boothroyd, and D. Prabhakaran, D. González, and M. Enderle, Phys. Rev. B **66**, 212405 (2002).
- [8] M. Hücker, M. v. Zimmermann, R. Klingeler, S. Kiele, J. Geck, S.N. Bakehe, J.Z. Zhang, J.P. Hill, A. Revcolevschi, D.J. Buttrey, B. Büchner, and J.M. Tranquada, Phys. Rev. B **74**, 085112 (2006).
- [9] S.A. Kivelson, I.P. Bindloss, E. Fradkin, V. Oganessian, J.M. Tranquada, A. Kapitulnik, and C. Howald, Rev. Mod. Phys. **75**, 1201 (2003).
- [10] M. Raczkowski, R. Frésard, and A.M. Oleś, Phys. Rev. B **73**, 174525 (2006).
- [11] M. Raczkowski, D. Poilblanc, R. Frésard, and A.M. Oleś, Phys. Rev. B **75**, 094505 (2007).
- [12] M. Raczkowski, R. Frésard, and A.M. Oleś, Phys. Rev. B **73**, 094429 (2006).
- [13] A.P. Ramirez, P.L. Gammel, S.-W. Cheong, D.J. Bishop, and P. Chandra, Phys. Rev. Lett. **76**, 447 (1996).
- [14] S.-W. Cheong, H.Y. Hwang, C.H. Chen, B. Batlogg, L.W. Rupp, Jr., and S.A. Carter, Phys. Rev. B **49**, 7088 (1994).
- [15] T. Katsufuji, T. Tanabe, T. Ishikawa, Y. Fukuda, T. Arima, and Y. Tokura, Phys. Rev. B **54**, R14230 (1996).
- [16] M. Hücker, M. v. Zimmermann, and G.D. Gu, Phys. Rev. B **75**, 041103(R) (2007).
- [17] J. Zaanen and P.B. Littlewood, Phys. Rev. B **50**, 7222 (1994).
- [18] S. Yamamoto, T. Fujiwara, and Y. Hatsugai, Phys. Rev. B **76**, 165114 (2007).
- [19] U. Schwingenschlögl, C. Schuster, and R. Frésard, Europhys. Lett. **81**, 27002 (2008).
- [20] T. Hotta and E. Dagotto, Phys. Rev. Lett. **92**, 227201 (2004).
- [21] Y. Takeda, R. Kanno, M. Sakano, O. Yamamoto, M. Takano, Y. Bando, H. Akinaga, K. Takita, and J.B. Goodenough, Mater. Res. Bull. **25**, 293 (1990).
- [22] P. Blaha, K. Schwarz, G. Madsen, D. Kvasnicka, and J. Luitz, *Wien2k: An augmented plane wave + local orbitals program for calculating crystal properties*, Vienna University of Technology, 2001.
- [23] U. Schwingenschlögl and C. Schuster, Europhys. Lett. **81**, 17007 (2008); Europhys. Lett. **81**, 26001 (2008).
- [24] U. Schwingenschlögl and C. Schuster, Phys. Rev. Lett. **99**, 237206 (2007); Europhys. Lett. **79**, 27003 (2007).
- [25] J.P. Perdew, K. Burke, and M. Ernzerhof, Phys. Rev. Lett. **77**, 3865 (1996).
- [26] V.I. Anisimov, I.V. Solovyev, M.A. Korotin, M.T. Czyzyk, and G.A. Sawatzky, Phys. Rev. B **48**, 16929 (1993).
- [27] A.I. Lichtenstein, V.I. Anisimov, and J. Zaanen, Phys. Rev. B **52**, R5467 (1995).
- [28] R.J. Cava, B. Batlogg, T.T. Palstra, J.J. Krajewski, W.F. Peck, Jr., A.P. Ramirez, and L.W. Rupp, Jr., Phys. Rev. B **43**, 1229 (1991).
- [29] J. Rodriguez-Carvajal, M.T. Fernandez-Diaz, and J.L. Martinez, J. Phys.: Condens. Matter **3**, 3215 (1991).
- [30] Y.-J. Kim, G.D. Gu, T. Gog, and D. Casa, Phys. Rev. B **77**, 064520 (2008).
- [31] V.I. Anisimov and O. Gunnarsson, Phys. Rev. B **43**, 7570 (1991).
- [32] V.I. Anisimov, D. Bukhvalov, and T.M. Rice, Phys. Rev. B **59**, 7901 (1999).